

Fractional Electron Loss in Approximate DFT and Hartree–Fock Theory

Michael J. G. Peach,[†] Andrew M. Teale,^{‡,§} Trygve Helgaker,[§] and David J. Tozer^{*,||}

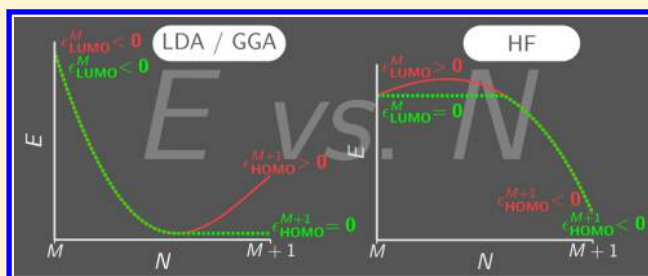
[†]Department of Chemistry, Lancaster University, Lancaster LA1 4YB, United Kingdom

[‡]School of Chemistry, University of Nottingham, Nottingham NG7 2RD, United Kingdom

[§]Department of Chemistry, Centre for Theoretical and Computational Chemistry, University of Oslo, P.O. Box 1033, Blindern, Oslo N-0315, Norway

^{||}Department of Chemistry, Durham University, South Road, Durham DH1 3LE, United Kingdom

ABSTRACT: Plots of electronic energy vs electron number, determined using approximate density functional theory (DFT) and Hartree–Fock theory, are typically piecewise convex and piecewise concave, respectively. The curves also commonly exhibit a minimum and maximum, respectively, in the neutral \rightarrow anion segment, which lead to positive DFT anion HOMO energies and positive Hartree–Fock neutral LUMO energies. These minima/maxima are a consequence of using basis sets that are local to the system, preventing fractional electron loss. Ground-state curves are presented that illustrate the idealized behavior that would occur if the basis set were to be modified to enable fractional electron loss without changing the description in the vicinity of the system. The key feature is that the energy cannot increase when the electron number increases, so the slope cannot be anywhere positive, meaning frontier orbital energies cannot be positive. For the convex (DFT) case, the idealized curve is flat beyond a critical electron number such that any additional fraction of an electron added to the system is unbound. The anion HOMO energy is zero. For the concave (Hartree–Fock) case, the idealized curve is flat up to some critical electron number, beyond which it curves down to the anion energy. A minimum fraction of an electron is required before any binding occurs, but beyond that, the full fraction abruptly binds. The neutral LUMO energy is zero. Approximate DFT and Hartree–Fock results are presented for the $F \rightarrow F^-$ segment, and results approaching the idealized behavior are recovered for highly diffuse basis sets. It is noted that if a DFT calculation using a highly diffuse basis set yields a negative LUMO energy then a fraction of an electron must bind and the electron affinity must be positive, irrespective of whether an electron binds experimentally. This is illustrated by calculations on $Ne \rightarrow Ne^-$.



INTRODUCTION

In recent years, there has been significant interest^{1–18} in the variation of the electronic energy, E , as a function of electron number, N , due to the relevance of this process to the calculation of quantities such as charge-transfer excitation energies,¹⁹ band gaps,⁶ and molecular dissociation energies^{1,2,20} in Kohn–Sham density functional theory (DFT) and Hartree–Fock theory. The exact E vs N behavior²¹ comprises a series of straight line segments with derivative discontinuities at the integers, with slopes on either side of an integer equal to the negative of the exact vertical ionization potential and electron affinity of the integer system. It is now well-established that the deficiencies inherent to approximate DFT and Hartree–Fock theory mean that this piecewise linearity is not recovered by practical calculations. Local DFT exchange–correlation functionals such as the local density approximation (LDA) or generalized gradient approximations (GGAs) instead exhibit piecewise convex curves; the energies are usually reasonable at integer electron number, but they are underestimated at noninteger. This deficiency has been termed^{1–4,9,22,23} many-electron self-interaction error or delocalization error, and it has significant implications for the

mentioned quantities. Hartree–Fock theory instead yields piecewise concave curves. It follows that hybrid functionals, which comprise a linear combination of GGA and exact exchange, yield curves that are intermediate between GGA and Hartree–Fock. The most accurate (minimum curvature) results are often obtained using range-separated exchange–correlation functionals, which provide a more sophisticated mechanism for including exact exchange.

The slope of an E vs N curve is related to the orbital energies.^{6,24,25} For DFT calculations using explicit density functionals such as LDA and GGA, the limiting values of $\frac{\partial E}{\partial N}$ on the electron-deficient and -abundant sides of an integer M are the HOMO energy, ϵ_H^M , and the LUMO energy, ϵ_L^M , of the M -electron system

$$\lim_{\delta \rightarrow 0} \frac{\partial E}{\partial N} \Big|_{M-\delta} = \epsilon_H^M \quad (1)$$

Received: August 21, 2015

Published: October 2, 2015

$$\lim_{\delta \rightarrow 0} \left. \frac{\partial E}{\partial N} \right|_{M+\delta} = \epsilon_L^M \quad (2)$$

Equations 1 and 2 are also satisfied for DFT calculations using orbital-dependent hybrid and range-separated functionals, when the usual generalized Kohn–Sham (GKS) formalism is used, and they are also satisfied for Hartree–Fock theory. If an optimized effective potential (OEP) formalism is instead used for orbital-dependent functionals, then an additional derivative discontinuity term must be introduced, as discussed in ref 6. In the present study, we focus on LDA and a range-separated functional within the GKS formalism, together with Hartree–Fock theory, meaning eqs 1 and 2 are valid throughout. These relationships are central to understanding the charge-transfer¹⁹ and band gap⁶ problems, and they form the basis of DFT tuning approaches,²⁶ whereby an exchange-correlation functional is constrained to yield frontier orbital energies equal to ionization potentials and/or electron affinities.

Many E vs N curves have been presented in the literature.^{1–12,14,15,18} In addition to the aforementioned deviation from piecewise linearity, it is common for LDA/GGA curves to exhibit an energy minimum in the segment connecting the neutral to anion and for Hartree–Fock curves to exhibit an energy maximum in that segment; for specific examples, see refs 1–7, 9–12, 14, and 15. In the present study, we highlight the fact that these minima/maxima are a consequence of using basis sets that are local to the system and that they cannot persist if fractional electron loss is possible. The analysis provides a simple perspective for understanding a range of issues in approximate DFT and Hartree–Fock theory, relating to electron binding, orbital energies, and electron affinities, as well as providing some unexpected findings. All calculations were performed in an unrestricted manner using the CADPAC²⁷ and Gaussian09²⁸ programs.

RESULTS AND DISCUSSION

Convex E vs N . Figure 1a presents schematic ground-state E vs N curves for a neutral system that vertically binds an electron, i.e., where the energy of the anion is below that of the neutral. We consider the region $M \leq N \leq M + 1$, where M is the electron number of the neutral system and $M + 1$ is the electron number of the anion. The red solid curve shows the convex behavior with an energy minimum that is often observed when LDA/GGA is used with a basis set that is local to the system (hereafter termed a local basis set). The limiting slope on the electron-abundant side of integer M is negative, so it follows from eq 2 that the LUMO energy of the neutral is $\epsilon_L^M < 0$, which is well-known. The energy drops to a minimum value at some critical electron number, N_c , but then increases again. The limiting slope on the electron-deficient side of the integer $M + 1$ is positive, so it follows from the $(M + 1)$ -electron analogue of eq 1 that the HOMO energy of the anion is $\epsilon_H^{M+1} > 0$. It is well-known that LDA/GGA HOMO energies of anions are often positive, and there has been significant discussion^{29–35} in the literature about the formal and practical implications of this. Figure 1a illustrates its origin from an E vs N perspective.

The presence of the minimum means that the energy of systems with electron number $N_c < N \leq M + 1$ is greater than that of the system with electron number N_c . For these systems, the energy could, in principle, be lowered by reducing the electron number in the vicinity of the system to N_c with the remaining fraction moving far from the system with zero energy. However, the use of a local basis set means that all of the electrons are

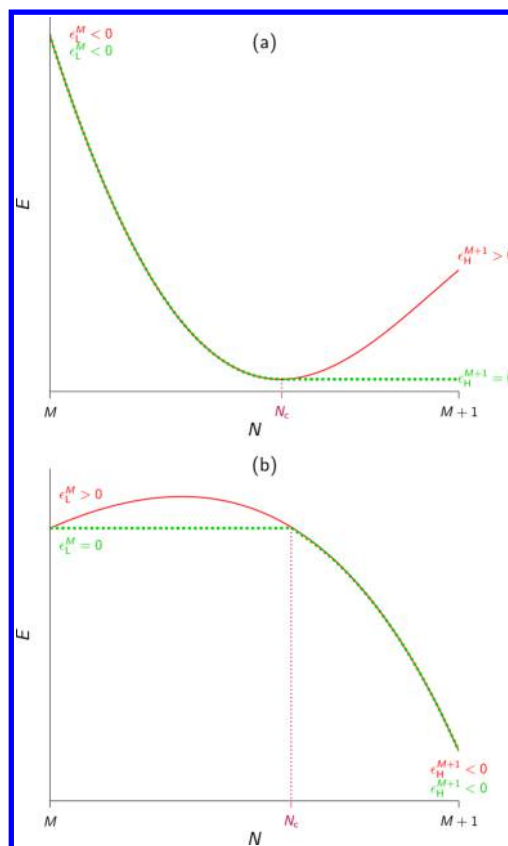


Figure 1. E vs N curves for a neutral system that vertically binds an electron. (a) A convex curve exhibiting an energy minimum (e.g., LDA/GGA). (b) A concave curve exhibiting an energy maximum (e.g., Hartree–Fock). Red solid curves indicate schematic curves determined using a local basis set. Green dotted curves indicate idealized curves that would be obtained if the basis set were to be modified to enable fractional electron loss without changing the description in the vicinity of the system.

constrained to be in the vicinity of the system, so this does not occur.

The green dotted curve in Figure 1a shows the idealized behavior that would occur if the basis set were to be modified to enable fractional electron loss without changing the description in the vicinity of the system. For systems with electron number $N_c < N \leq M + 1$, the variational ground-state solution is obtained by binding only N_c electrons and moving the remaining fraction far from the system. The energy of all of these systems is the same as the energy of the system with electron number N_c , so the curve is flat, exhibiting a degenerate minimum, and $\epsilon_H^{M+1} = 0$. The electron affinity of the neutral system ($A^M = E(M) - E(M + 1)$) is larger than it was from the red curve, which is somewhat nonintuitive given that the increase in affinity is associated with fractional electron loss. Several studies^{29–35} have discussed fractional electron loss, anion HOMOs approaching zero, and increased electron affinities, although the tendency has been to consider the issues from the perspective of the exchange-correlation potential. Figure 1a illustrates all of these aspects from the perspective of an E vs N curve. It also demonstrates that a positive anion HOMO energy simply reflects the inability to lose a fraction of an electron, due to a local basis set.

The shape of the idealized curve in Figure 1a highlights a key result: when electron loss is possible, the E vs N curve satisfies $E(N + \delta) \leq E(N)$, for $\delta \geq 0$, i.e., the energy cannot increase when

the electron number increases and the slope of the curve cannot be anywhere positive.

The idealized electron addition process is, therefore, as follows: As the electron number increases from M to N_c , all of the added fraction binds. Once the electron number exceeds N_c , however, the number in the vicinity of the system does not change, and the remaining fraction is unbound. The anion has only N_c electrons in the vicinity of the system, with the remaining $M + 1 - N_c$ electrons unbound.

In principle, curves exhibiting the idealized green curve behavior in Figure 1a could be obtained by augmenting a standard atom-centered Gaussian basis set with basis functions located a long way from the system, which would enable fractional electron loss without changing the description in the vicinity of the system. In practical calculations, however, fractional electron loss is usually facilitated (to some extent) by adding diffuse basis functions centered on or close to the nuclei. The addition of these functions inevitably affects the description in the vicinity of the system, so the idealized behavior in Figure 1a will not be exactly reproduced. The unique minimum must vanish when the basis set is sufficiently diffuse, but different basis sets will yield different values of N_c , and we cannot rule out the possibility that the lowest energy will occur at the anion, giving a negative $\epsilon_{\text{H}}^{M+1}$.

To investigate the behavior in real calculations, we consider the $\text{F} \rightarrow \text{F}^-$ segment ($M = 9$) using a series of basis sets of increasing diffuseness. Specifically, we augment the standard cc-pVTZ basis set with np functions, reflecting the symmetry of the orbital whose occupation is changing, with exponents obtained from a geometric progression based on the ratio of the p exponents in cc-pVTZ and aug-cc-pVTZ. (The basis sets are, therefore, equivalent to the regular augmented sets of Woon and Dunning,³⁶ but they omit the s , d , and f diffuse functions.) We denote the basis sets cc-pVTZ+ np , where $n = 0-5$. Figure 2 presents E vs N curves determined using the LDA functional^{37,38} for the six basis sets. The curves were determined by evaluating the electronic energy for a set of equally spaced N values, with increment 0.05; unless otherwise stated, the same increment is used throughout the study. The cc-pVTZ basis set, with no diffuse functions, exhibits strong curvature and a pronounced minimum. The remaining curves are almost indistinguishable on this scale. The lower plot expands the shaded area. All of the curves exhibit a minimum, although it becomes less pronounced with increasing diffuseness, approaching the idealized flattening in Figure 1a.

To investigate the loss of a fraction of an electron, Figure 3 compares the quantity $z^2\phi_{\text{HOMO}}^2$, where ϕ_{HOMO} is the $2p_z/\beta\text{HOMO}$, for $N = N_c = 9.87$ and $N = M + 1 = 10$, determined using LDA with the most diffuse cc-pVTZ+5p basis set. On the full scale, the two orbitals are virtually indistinguishable. However, close inspection reveals that at $N = 10$ the orbital acquires non-negligible character at very large distances, reflecting the loss of a fraction of an electron, which is not present when $N = 9.87$.

Table 1 lists the values of the LDA neutral LUMO energy, anion HOMO energy, and electron affinity of the neutral. As the basis set becomes more diffuse, the neutral LUMO energy is negative and stable, the anion HOMO energy reduces from a positive value toward zero, and the affinity increases, consistent with Figures 1 and 2. We note that a good estimate of the limiting electron affinity can be obtained from a knowledge of just the minimum of the E vs N curve, without requiring an explicit

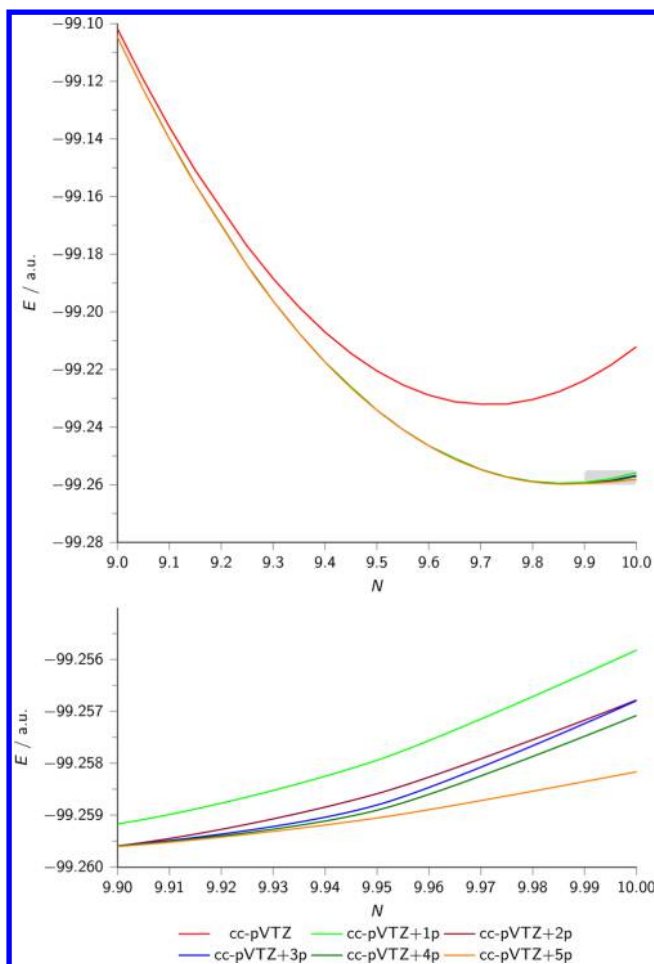


Figure 2. E vs N curves for the $\text{F} \rightarrow \text{F}^-$ segment, determined using LDA. The lower plot expands the shaded area.

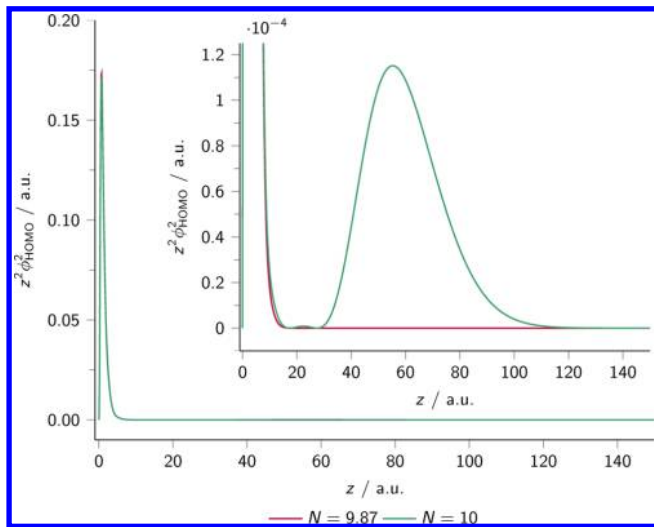


Figure 3. Plots of $z^2\phi_{\text{HOMO}}^2$ for selected values of N , in the $\text{F} \rightarrow \text{F}^-$ segment, determined using LDA with the cc-pVTZ+5p basis set. Note that the inset plot has a smaller vertical scale.

calculation on the anion, which can be difficult to converge with highly diffuse basis sets.

Jarecki and Davidson³² performed a detailed investigation into the HOMO energy of the F^- anion, highlighting the importance of ensuring high accuracy with diffuse basis functions and low

Table 1. LUMO Energy of F, HOMO Energy of F^- , and Electron Affinity of F Determined Using LDA, Hartree–Fock (HF), and CAM-B3LYP^a

	LDA			HF			CAM-B3LYP		
	ϵ_L^M	ϵ_H^{M+1}	A^M	ϵ_L^M	ϵ_H^{M+1}	A^M	ϵ_L^M	ϵ_H^{M+1}	A^M
cc-pVTZ	−0.366	0.142	3.00	0.067	−0.135	0.58	−0.20	0.01	2.51
cc-pVTZ+1p	−0.377	0.051	3.33	0.035	−0.180	1.19	−0.21	0.01	3.52
cc-pVTZ+2p	−0.377	0.044	4.14	0.026	−0.180	1.19	−0.21	−0.07	3.53
cc-pVTZ+3p	−0.377	0.043	4.14	0.012	−0.180	1.19	−0.21	−0.07	3.53
cc-pVTZ+4p	−0.377	0.028	4.15	0.004	−0.180	1.19	−0.21	−0.07	3.53
cc-pVTZ+5p	−0.377	0.013	4.18	0.001	−0.180	1.19	−0.21		

^aOrbital energies are in au, and electron affinities are in eV.

electron densities. They found that the LDA HOMO energy was negative when extremely diffuse functions were added to a quintuple-zeta basis. We have ensured that our calculations accurately treat diffuse basis functions and low densities. The fact that the two studies yield different signs for the HOMO energy simply reflects the different underlying basis sets used. A negative HOMO energy is not inconsistent with the analysis in the present study (see above).

Concave E vs N . Next, we extend the analysis to concave curves with an energy maximum. Figure 1b again presents schematic ground-state E vs N curves for a neutral system that binds an electron. The red solid curve now shows the concave behavior that is often observed when Hartree–Fock theory is used with a local basis set. The limiting slope on the electron-abundant side of integer M is now positive, meaning that $\epsilon_L^M > 0$, which is well-known. The energy increases to a maximum value and then decreases, becoming equal to the energy of the M -electron system at some critical electron number, N_c . Beyond this, the energy curves down to the energy of the $(M + 1)$ -electron system. The limiting slope on the electron-deficient side of the integer $M + 1$ is now negative, meaning that $\epsilon_H^{M+1} < 0$, as is again well-known. In analogy to Figure 1a, systems with $M < N < N_c$ could, in principle, lower their energy by reducing the electron number in the vicinity of the system to M ; however, the use of a local basis set again prevents this.

The green dotted curve in Figure 1b shows the idealized behavior that would occur if fractional electron loss was possible without changing the description in the vicinity of the system. For systems with electron number $M < N < N_c$, the variational ground-state solution is obtained by binding only M electrons and moving the remaining fraction far from the system. The energy of all of these systems is the same as the energy of the M -electron system, so the curve is flat, exhibiting a degenerate minimum, and $\epsilon_L^M = 0$. This provides a simple explanation as to why Hartree–Fock LUMO energies approach zero as the basis sets become more diffuse (e.g., see refs 39 and 40). It also demonstrates that a positive neutral LUMO energy simply reflects the inability to lose a fraction of an electron, due to a local basis set.

The idealized electron addition process is, therefore, as follows: As the electron number increases from M to N_c , all of the added fraction is unbound, leaving only M electrons in the vicinity of the system. At the point where the electron number exceeds N_c , all electrons bind, meaning there is an abrupt shift of $N_c - M$ electrons from far away to the vicinity of the system, with no change in electronic energy. As the electron number is further increased, all of the additional added fraction binds. The anion has all $M + 1$ electrons in the vicinity of the system.

Figure 4 presents E vs N curves for $F \rightarrow F^-$, determined using Hartree–Fock theory with the same cc-pVTZ+ np basis sets. The

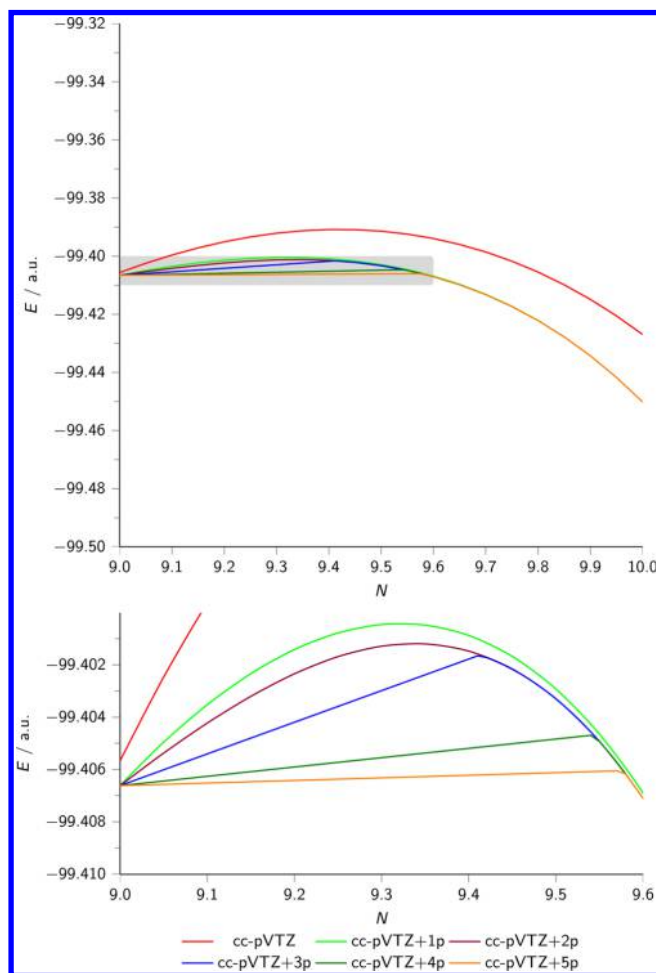


Figure 4. E vs N curves for the $F \rightarrow F^-$ segment, determined using Hartree–Fock theory. The lower plot expands the shaded area.

cc-pVTZ curve exhibits strong curvature with a pronounced maximum. The lower plot expands the shaded region. With increasing diffuseness, the curves do, indeed, flatten, approaching the idealized behavior in Figure 1b. Note that for the three most diffuse basis sets an electron number increment of 0.01 was used in order to ensure that the shape is faithfully reproduced.

To investigate the abrupt shift of $N_c - M$ electrons from far away to the vicinity of the atom at N_c electrons, Figure 5 again plots $z^2\phi_{\text{HOMO}}^2$, but this time at electron numbers on either side of $N = N_c = 9.58$, determined using Hartree–Fock theory with the cc-pVTZ+5p basis set. The entire orbital shifts from very large distance to the vicinity of the atom as the electron number increases through N_c , precisely as predicted. The origin of this

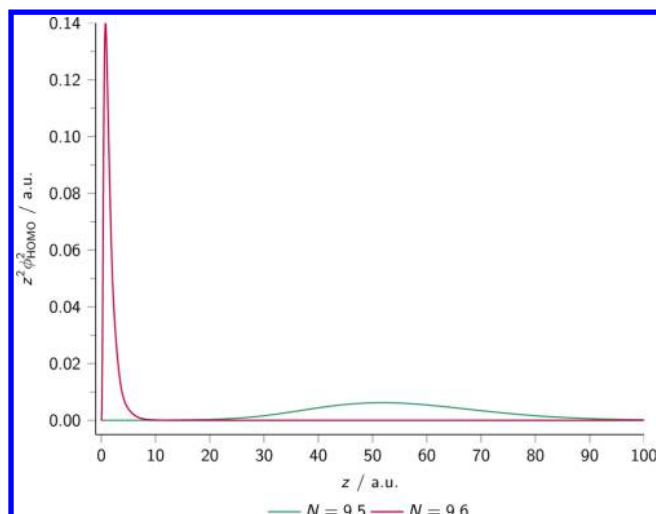


Figure 5. Plots of $z^2 \phi_{\text{HOMO}}^2$, for selected values of N , in the $F \rightarrow F^-$ segment, determined using Hartree–Fock theory with the cc-pVTZ+5p basis set.

behavior is evident from Figure 6, which plots the energies of the two lowest solutions obtained from the Hartree–Fock

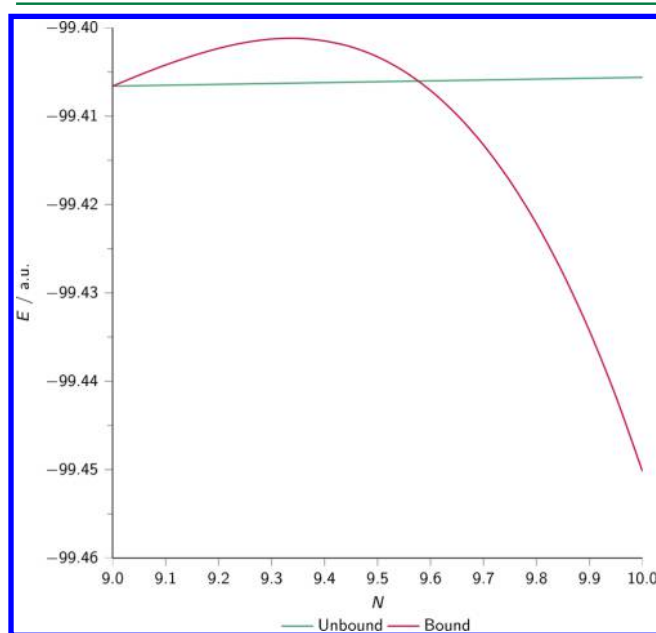


Figure 6. E vs N curves for the two lowest energy solutions, in the $F \rightarrow F^-$ segment, determined using Hartree–Fock theory, with the cc-pVTZ+5p basis set.

calculations, as a function of N , for the cc-pVTZ+5p basis set. The state denoted bound is the state where the orbital being occupied is localized in the vicinity of the atom; the state labeled unbound is the state where the orbital being occupied is located far from the atom. The E vs N curve in Figure 4 is obtained by choosing the lower of the bound and unbound energies at each electron number. The state crossing at $N = N_0$, therefore, explains the shape of the curve in Figure 4 and the shift of electrons in Figure 5.

Table 1 lists the values of the Hartree–Fock orbital energies and electron affinities. As the basis set becomes more diffuse, the neutral LUMO reduces from a positive value toward zero and the anion HOMO is negative and stable. Unlike in the LDA case, the

affinities are stable with respect to basis set. This is consistent with Figures 1 and 4.

Range-Separated Exchange–Correlation Functionals.

The curves in Figure 2 were determined using LDA, and we have verified that similar behavior is obtained using a GGA functional (specifically, BLYP^{37,41,42}). As noted in the Introduction, curves from a hybrid functional would be intermediate between GGA and Hartree–Fock curves, depending on the amount of orbital exchange. Before completing our analysis of $F \rightarrow F^-$, we comment on the performance of range-separated functionals, since these have been shown to successfully reduce the curvature. Figure 7 and Table 1 show results determined using the CAM-

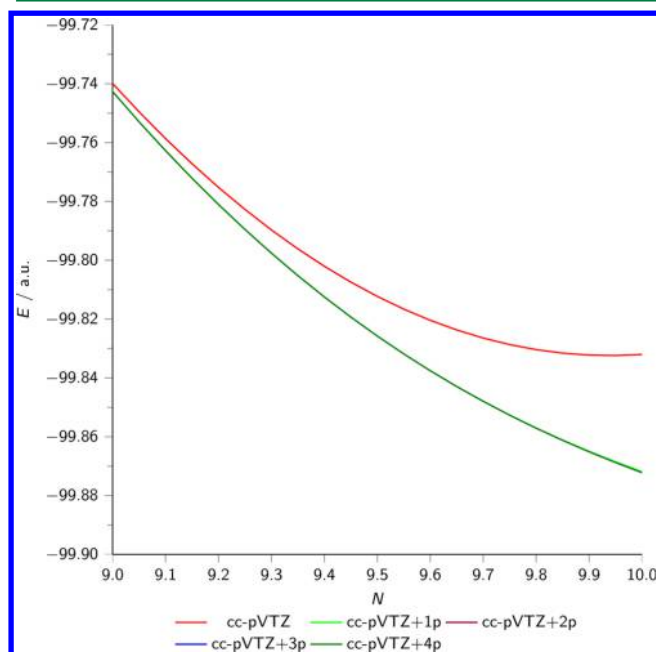


Figure 7. E vs N curves for the $F \rightarrow F^-$ segment, determined using CAM-B3LYP.

B3LYP functional⁴³ (results using the cc-pVTZ+5p basis set are not included due to convergence problems). The three most diffuse basis sets have the lowest energy at the anion, with no tendency toward leveling out/fractional electron loss; the anion HOMO energies are negative.

It is also pertinent to note that the parameters in range-separated functionals are sometimes determined by tuning the functional to approximately recover Koopmans conditions, either on a system-by-system basis²⁶ or through a parametrized functional.⁴⁴ The aforementioned observations regarding energy curvature, frontier orbital energies, and electron affinities are pertinent to such approaches, so it is important that the effect of diffuse functions is correctly taken into account, particularly when the electron affinity is involved.

Implications of a Negative LUMO Energy. Consider an idealized DFT calculation on a neutral M -electron system, for which fractional electron loss is possible. If the LUMO energy is negative, then the E vs N curve must initially drop as a fraction of an electron is added to the M -electron system (the initial slope is negative; see eq 2). However, as discussed above, further increasing N cannot lead to an increase in the energy. It follows that a nonzero fraction of an electron must bind, and the energy of the anion must be below that of the neutral, meaning that the electron affinity must be positive, irrespective of whether the

electron vertically binds in reality. To test this, we have performed calculations on the $\text{Ne} \rightarrow \text{Ne}^-$ segment ($M = 10$), which represents an extreme case where no binding should be observed. The LUMO energy in Ne is much more sensitive to basis set than it is in the F atom (3s vs 2p), and the use of an analogous cc-pVTZ+ ns basis set, where s rather than p functions are added due to the new symmetry, does not actually yield a negative LUMO energy. We therefore instead present results obtained using an even more extensive aug-cc-pVTZ+ ns basis set, obtained by adding additional s diffuse functions to aug-cc-pVTZ, using a geometric progression based on the ratio of the s exponents in aug-cc-pVTZ and d-aug-cc-pVTZ.

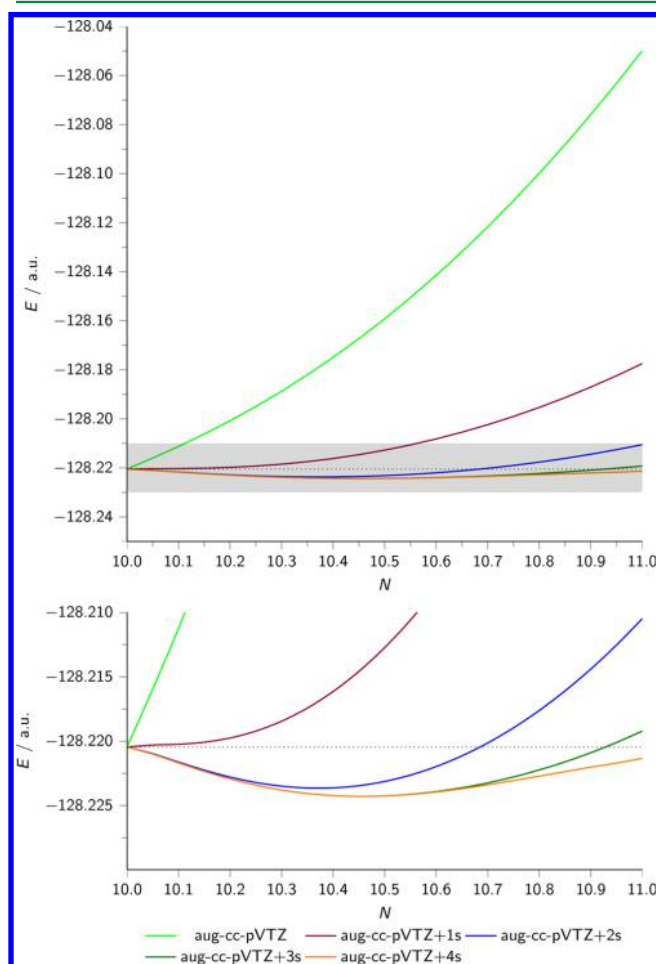


Figure 8. E vs N curves for the $\text{Ne} \rightarrow \text{Ne}^-$ segment, determined using LDA. The lower plot expands the shaded area.

Figure 8 presents the LDA E vs N curves, and Table 2 lists the corresponding neutral LUMO energy, anion HOMO energy, and electron affinity of the neutral. The LUMO energy is positive for the first two basis sets, but it is negative for the latter three, meaning that three E vs N curves drop as the electron number increases beyond 10. Of these, the aug-cc-pVTZ+2s and aug-cc-pVTZ+3s basis sets are not sufficiently diffuse for the flattening to give an anion energy below that of the neutral, meaning the electron affinity is negative. However, for the most diffuse aug-cc-pVTZ+4s basis set, the flattening is sufficiently pronounced that the anion energy is below that of the neutral and the electron affinity is positive, as in the idealized case. We have confirmed that the same behavior is observed using the BLYP GGA.

We emphasize that this noble gas atom is an extreme case, where the LUMO energy is particularly sensitive to basis set. For many closed-shell systems, the LUMO is appreciably more negative, and the effect will be more pronounced. For example, we previously⁴⁵ performed calculations on C_2H_4 using a highly diffuse augmented cc-pVTZ basis set, for which the LUMO energy was more than an order of magnitude more negative than in this Ne example. We observed that the electron affinity of the molecule was positive, despite the fact that it does not vertically bind an electron experimentally. The above analysis explains the origin of that positive affinity.

As discussed and illustrated earlier in this study, it is well-established^{29–35} that when a highly diffuse basis set is used approximate DFT functionals can fail to bind a full electron in cases where it should bind. We now expand that statement to add that if the DFT LUMO energy is negative then it will incorrectly bind a fraction of an electron and exhibit a positive electron affinity in cases where it should not bind!

Finally, Table 2 lists the orbital energies and electron affinities determined using Hartree–Fock theory and CAM-B3LYP. For Hartree–Fock, the LUMO energy is positive for all of the basis sets, and the electron affinity approaches zero from below. For CAM-B3LYP, the aug-cc-pVTZ+4s basis set does yield a negative LUMO, but the flattening of the E vs N curve (not shown) is not sufficient to yield a positive affinity. Neither Hartree–Fock theory nor the CAM-B3LYP functional, therefore, predict electron binding or a positive affinity, in agreement with experiment.

CONCLUSIONS

In this study, we highlighted the fact that minima/maxima in E vs N curves from approximate DFT and Hartree–Fock theory are a consequence of using basis sets that are local to the system, preventing fractional electron loss. This is distinct from the underlying convexity/concavity of the curves, which arises due to the inherent deficiencies in the electronic structure methods.

Table 2. LUMO Energy of Ne, HOMO Energy of Ne^- , and Electron Affinity of Ne Determined Using LDA, Hartree–Fock (HF), and CAM-B3LYP^a

	LDA			HF			CAM-B3LYP		
	ϵ_L^M	ϵ_H^{M+1}	A^M	ϵ_L^M	ϵ_H^{M+1}	A^M	ϵ_L^M	ϵ_H^{M+1}	A^M
aug-cc-pVTZ	0.089	0.272	−4.64	0.201	0.198	−5.44	0.134	0.216	−4.77
aug-cc-pVTZ+1s	0.009	0.102	−1.17	0.055	0.054	−1.48	0.028	0.068	−1.24
aug-cc-pVTZ+2s	−0.002	0.043	−0.27	0.015	0.015	−0.41	0.006	0.024	−0.32
aug-cc-pVTZ+3s	−0.003	0.019	−0.03	0.004	0.004	−0.12	0.000	0.009	−0.08
aug-cc-pVTZ+4s	−0.003	0.008	0.02	0.001	0.001	−0.03	−0.001	0.004	−0.01

^aOrbital energies are in au, and electron affinities are in eV.

Ground-state E vs N curves were presented that illustrate the idealized behavior that would occur if fractional electron loss was possible without changing the description in the vicinity of the system. The key feature is that $E(N + \delta) \leq E(N)$, for $\delta \geq 0$, i.e., the energy cannot increase when the electron number increases. It follows that the slope of the E vs N curve cannot be anywhere positive, so from eqs 1 and 2, the frontier orbital energies cannot be positive. Approximate DFT and Hartree–Fock calculations were presented for $F \rightarrow F^-$, and results approaching the idealized behavior were recovered. Calculations on $Ne \rightarrow Ne^-$ verified that for highly diffuse basis sets a negative LUMO must lead to a positive electron affinity.

Ground-state E vs N curves, frontier orbital energies, and electron affinities are important throughout contemporary DFT. This study contributes to the understanding of these quantities.

AUTHOR INFORMATION

Corresponding Author

*E-mail: d.j.tozer@durham.ac.uk.

Funding

D.J.T. and M.J.G.P. thank the EPSRC for financial support (EP/G06928X/1). T.H. and A.M.T. thank the Norwegian Research Council through the CoE Centre for Theoretical and Computational Chemistry (CTCC) grant number 179568/V30 and through the European Research Council under the European Union Seventh Framework Program through the Advanced Grant ABACUS, ERC grant agreement number 267683. A.M.T. is grateful for support from the Royal Society University Research Fellowship scheme.

Notes

The authors declare no competing financial interest.

REFERENCES

- (1) Mori-Sánchez, P.; Cohen, A. J.; Yang, W. *J. Chem. Phys.* **2006**, *125*, 201102.
- (2) Ruzsinszky, A.; Perdew, J. P.; Csonka, G. I.; Vydrov, O. A.; Scuseria, G. E. *J. Chem. Phys.* **2007**, *126*, 104102.
- (3) Vydrov, O. A.; Scuseria, G. E.; Perdew, J. P. *J. Chem. Phys.* **2007**, *126*, 154109.
- (4) Cohen, A. J.; Mori-Sánchez, P.; Yang, W. *J. Chem. Phys.* **2007**, *126*, 191109.
- (5) Teale, A. M.; De Proft, F.; Tozer, D. J. *J. Chem. Phys.* **2008**, *129*, 044110.
- (6) Cohen, A. J.; Mori-Sánchez, P.; Yang, W. *Phys. Rev. B: Condens. Matter Mater. Phys.* **2008**, *77*, 115123.
- (7) Mori-Sánchez, P.; Cohen, A. J.; Yang, W. *Phys. Rev. Lett.* **2008**, *100*, 146401.
- (8) Song, J.-W.; Watson, M. A.; Hirao, K. *J. Chem. Phys.* **2009**, *131*, 144108.
- (9) Haunschild, R.; Henderson, T. M.; Jiménez-Hoyos, C. A.; Scuseria, G. E. *J. Chem. Phys.* **2010**, *133*, 134116.
- (10) Tsuneda, T.; Song, J.-W.; Suzuki, S.; Hirao, K. *J. Chem. Phys.* **2010**, *133*, 174101.
- (11) Körzdörfer, T.; Parrish, R. M.; Sears, J. S.; Sherrill, C. D.; Brédas, J.-L. *J. Chem. Phys.* **2012**, *137*, 124305.
- (12) Srebro, M.; Autschbach, J. *J. Phys. Chem. Lett.* **2012**, *3*, 576.
- (13) Stein, T.; Autschbach, J.; Govind, N.; Kronik, L.; Baer, R. *J. Phys. Chem. Lett.* **2012**, *3*, 3740–3744.
- (14) Teale, A. M.; De Proft, F.; Geerlings, P.; Tozer, D. J. *Phys. Chem. Chem. Phys.* **2014**, *16*, 14420–14434.
- (15) Autschbach, J.; Srebro, M. *Acc. Chem. Res.* **2014**, *47*, 2592–2602.
- (16) Mori-Sánchez, P.; Cohen, A. J. *Phys. Chem. Chem. Phys.* **2014**, *16*, 14378–14387.
- (17) Vlček, V.; Eisenberg, H. R.; Steinle-Neumann, G.; Kronik, L.; Baer, R. *J. Chem. Phys.* **2015**, *142*, 034107.
- (18) Whittleton, S. R.; Sosa Vazquez, X. A.; Isborn, C. M.; Johnson, E. R. *J. Chem. Phys.* **2015**, *142*, 184106.
- (19) Tozer, D. J. *J. Chem. Phys.* **2003**, *119*, 12697–12699.
- (20) Bally, T.; Sastry, G. N. *J. Phys. Chem. A* **1997**, *101*, 7923–7925.
- (21) Perdew, J. P.; Parr, R. G.; Levy, M.; Balduz, J. L. *Phys. Rev. Lett.* **1982**, *49*, 1691–1694.
- (22) Dutoi, A. D.; Head-Gordon, M. *Chem. Phys. Lett.* **2006**, *422*, 230–233.
- (23) Ruzsinszky, A.; Perdew, J. P.; Csonka, G. I.; Vydrov, O. A.; Scuseria, G. E. *J. Chem. Phys.* **2006**, *125*, 194112.
- (24) Janak, J. F. *Phys. Rev. B: Condens. Matter Mater. Phys.* **1978**, *18*, 7165–7168.
- (25) Chan, G. K.-L. *J. Chem. Phys.* **1999**, *110*, 4710–4723.
- (26) Stein, T.; Kronik, L.; Baer, R. *J. Am. Chem. Soc.* **2009**, *131*, 2818–2820.
- (27) Amos, R. D. et al. *CADPAC 6.5*, The Cambridge Analytic Derivatives Package; Cambridge, England, 1998.
- (28) Frisch, M. J. et al. *Gaussian 09*, Revision A.02; Gaussian Inc.: Wallingford, CT, 2009.
- (29) Shore, H. B.; Rose, J. H.; Zaremba, E. *Phys. Rev. B* **1977**, *15*, 2858–2861.
- (30) Galbraith, J. M.; Schaefer, H. F., III. *J. Chem. Phys.* **1996**, *105*, 862–864.
- (31) Rösch, N.; Trickey, S. B. *J. Chem. Phys.* **1997**, *106*, 8940–8941.
- (32) Jarecki, A. A.; Davidson, E. R. *Chem. Phys. Lett.* **1999**, *300*, 44–52.
- (33) Jensen, F. J. *Chem. Theory Comput.* **2010**, *6*, 2726–2735.
- (34) Lee, D.; Furche, F.; Burke, K. *J. Phys. Chem. Lett.* **2010**, *1*, 2124–2129.
- (35) Kim, M.-C.; Sim, E.; Burke, K. *J. Chem. Phys.* **2011**, *134*, 171103.
- (36) Woon, D. E.; Dunning, T. H., Jr. *J. Chem. Phys.* **1994**, *100*, 2975–2988.
- (37) Dirac, P. A. M. *Math. Proc. Cambridge Philos. Soc.* **1930**, *26*, 376–385.
- (38) Vosko, S. H.; Wilk, L.; Nusair, M. *Can. J. Phys.* **1980**, *58*, 1200–1211.
- (39) Allen, M. J.; Tozer, D. J. *J. Chem. Phys.* **2000**, *113*, 5185–5192.
- (40) Baerends, E. J.; Gritsenko, O. V.; van Meer, R. *Phys. Chem. Chem. Phys.* **2013**, *15*, 16408–16425.
- (41) Becke, A. D. *Phys. Rev. A: At, Mol, Opt. Phys.* **1988**, *38*, 3098–3100.
- (42) Lee, C.; Yang, W.; Parr, R. G. *Phys. Rev. B: Condens. Matter Mater. Phys.* **1988**, *37*, 785–789.
- (43) Yanai, T.; Tew, D. P.; Handy, N. C. *Chem. Phys. Lett.* **2004**, *393*, 51–57.
- (44) Verma, P.; Bartlett, R. J. *J. Chem. Phys.* **2014**, *140*, 18A534.
- (45) Peach, M. J. G.; De Proft, F.; Tozer, D. J. *J. Phys. Chem. Lett.* **2010**, *1*, 2826–2831.